

# Purity Evaluation of As-Prepared Single-Walled Carbon Nanotube Soot by Use of Solution-Phase Near-IR Spectroscopy

M. E. Itkis, D. E. Perea, S. Niyogi, S. M. Rickard, M. A. Hamon, H. Hu, B. Zhao, and R. C. Haddon\*

*Center for Nanoscale Science and Engineering, Departments of Chemistry and Chemical & Environmental Engineering, University of California, Riverside, California 92521-0403*

*Received December 1, 2002; Revised Manuscript Received December 26, 2002*

## ABSTRACT

We report a rapid, quantitative procedure for the evaluation of the carbonaceous purity of bulk quantities of as-prepared single-walled carbon nanotube (SWNT) soot by the utilization of solution-phase near-IR spectroscopy. The procedure starts with two steps of homogenization followed by solution/dispersion spectroscopy of a representative part of the bulk sample. The purity is evaluated against a reference sample by utilizing the region of the second interband transition ( $S_{22}$ ) for semiconducting SWNTs. The procedure is found to be capable of reliably analyzing the carbonaceous purity of a 10-g batch of SWNTs produced by the electric arc discharge method to within 3%.

Single-walled carbon nanotubes (SWNTs) are a fascinating material with promising applications in nanoelectronics, field-emission displays, and nanostructural composites.<sup>1–3</sup> The realization of this potential will require a substantial improvement in the purity of the as-prepared (AP) SWNT material.<sup>4</sup> All currently known techniques for the production of SWNTs generate significant amounts of carbonaceous impurities, such as amorphous carbon and carbon nanoparticles, often with metal catalyst enclosed.<sup>5–7</sup> The current quoted purity of AP-SWNTs ranges from 10 to 70% depending on the method and source of production.<sup>5–9</sup> For most applications, the AP-SWNTs require a rigorous purification process.<sup>6,10–12</sup> In some cases the purification step is claimed to produce materials with purity levels above 90%; typically, this leads to an order of magnitude increase in the price of the purified material. In addition, most purification procedures modify the pristine AP-SWNTs by introducing chemical functionalities, doping, and defects.<sup>8,13–20</sup>

The electric arc discharge technique (EA) is a potential candidate for the large-scale commercial production of SWNTs.<sup>5</sup> Multiple parameters are involved in the operation of the EA process, such as the type of buffer gas and its pressure, the arc discharge current and gap voltage, the electrode preparation procedure and composition, choice of catalysts, arc chamber geometry, and electrode orientation.<sup>21–24</sup> An important goal of the research in this area is devoted to

finding a combination of parameters that minimizes the impurities produced in the process.

Figure 1a shows an SEM image of a fragment of the AP-SWNT soot collected from the arc chamber that shows almost no trace of impurities. This observation demonstrates the ability of the EA process to produce SWNTs with a high degree of perfection when all of the parameters of the process fortuitously match the ideal conditions for SWNT growth. Typically, EA-produced AP-SWNT soot contains a significant amount of impurities, and the average material collected from the arc chamber is usually very inhomogeneous, as can be seen in Figure 1b.

To reduce the impurities that are formed in the EA process, it is important to be able to monitor the purity of the AP-SWNTs as a function of the parameters of the arc process. This requires a quantitative measure of purity that can be scaled to evaluate bulk quantities of sample batches of any size. Although SEM and TEM methods are routinely used to evaluate the purity of SWNTs (Figure 1), the use of these methods for the quantitative evaluation of the purity of bulk samples is highly problematic. We estimate that the amount of material that can be seen and analyzed within one SEM frame (such as those shown in Figure 1) is less than  $10^{-12}$  g. It is virtually impossible to homogenize a 10-g batch of AP-SWNT soot to the level of  $10^{-12}$  g, which is what would be required to make 1 SEM frame or even 10 frames sufficiently representative to allow definitive conclusions

\* Corresponding author. E-mail: haddon@ucr.edu.

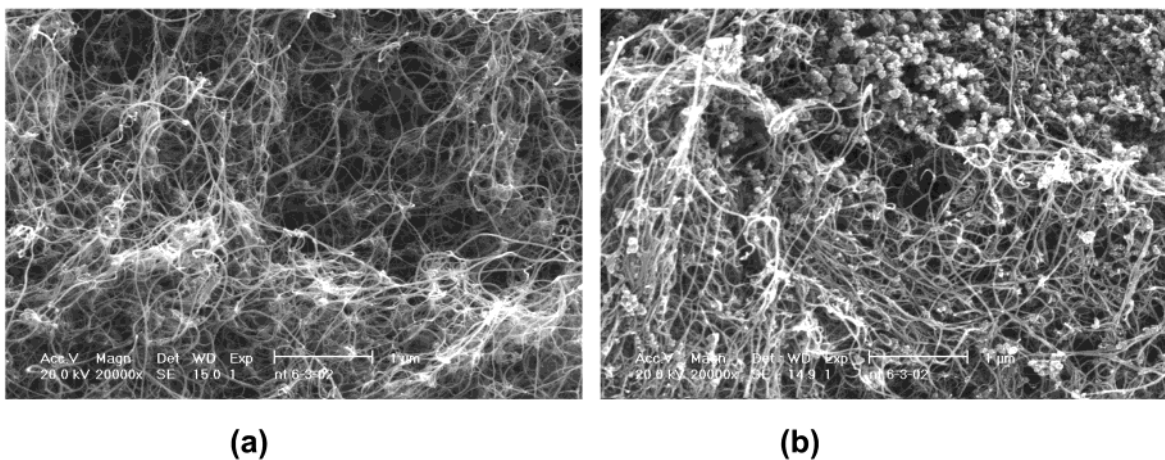


**Figure 1.** (a) SEM image of a fragment of high-purity AP-SWNT soot collected in the arc chamber that appears to consist almost solely of SWNTs without any visible traces of impurities. (b) SEM image of typical AP-SWNT soot with clearly observable impurities.

about the purity of the bulk sample to be drawn. Even under the assumption of representative SEM images, there is no algorithm that has been described in the literature that allows the quantitative evaluation of SWNT purity from SEM images such as those shown in Figure 1.

The impurities in AP-SWNTs may be divided into two categories: carbonaceous (amorphous carbon and graphitic nanoparticles) and metallic (typically transition-metal catalysts). Thermogravimetric analysis (TGA) has been successfully used to analyze the amount of metallic components quantitatively whereas Raman spectroscopy has been used to estimate qualitatively the carbonaceous impurities in AP- and purified-SWNTs.<sup>6,10,25–27</sup>

Near-infrared (NIR) spectroscopy has been established as an important tool for characterizing the electronic band structure of SWNTs.<sup>13,15,20,28–32</sup> Current synthetic techniques produce SWNTs with a range of chiralities and diameters, and this leads to a mixture of metallic and semiconducting SWNTs.<sup>1,33</sup> The semiconducting SWNTs give rise to a series of transitions between the principal mirror spikes in the electronic density of states (DOS) starting with  $S_{11} = 2a\beta/d$  and  $S_{22} = 4a\beta/d$  whereas the metallic SWNTs show their first transition at  $M_{11} = 6a\beta/d$ , where  $a$  is the carbon–carbon bond length (nm),  $\beta$  is the transfer integral between  $p\pi$  orbitals ( $\beta = \sim 2.9$  eV), and  $d$  is SWNT diameter (nm).<sup>1,33,34</sup> These interband transitions produce prominent features in the NIR spectral range, which can be used to analyze the SWNT type and diameter distribution<sup>31,32</sup> and the effects of doping.<sup>13,15,20,29,30</sup> We now show that solution-phase NIR spectroscopy can be used to provide a rapid, quantitative procedure for the evaluation of the carbonaceous purity of bulk quantities of as-prepared single-walled carbon nanotube (AP-SWNT) soot.

Figure 2a shows a typical absorption spectrum of a film of purified-SWNT material produced by the EA technique with a Ni/Y catalyst ratio of 4:1 atomic % after purification by nitric acid treatment followed by cross-flow filtration.<sup>6,35</sup> The film was prepared by spraying a SWNT dispersion in dimethylformamide (DMF) on a glass substrate heated to 160 °C.<sup>20</sup> The characteristic bands centered around 5500,

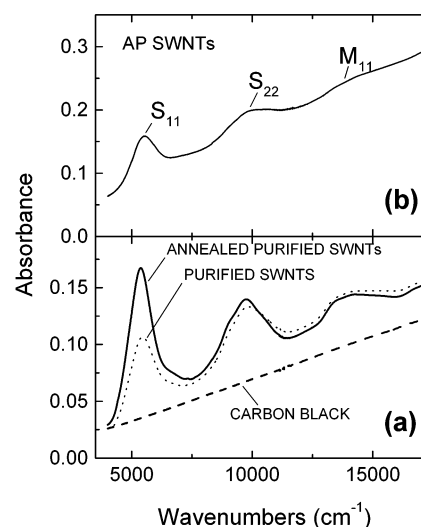


**Figure 2.** (a) NIR absorption spectra of thin films of carbon black (– –), purified SWNTs (· ·), and purified SWNTs after annealing in vacuum at 350 °C. (b) NIR absorption spectrum of a thin film of a random sample of EA-produced AP-SWNT soot.

9800, and 13 800  $\text{cm}^{-1}$  correspond to  $S_{11}$  and  $S_{22}$  interband transitions in the semiconducting SWNTs, and  $M_{11}$  corresponds to the interband transition in metallic SWNTs. The width and fine structure of these bands originate from the distribution of SWNT diameters and chiralities that are produced in the EA.<sup>5</sup> The electronic transition  $S_{11}$  is suppressed in the purified sample (Figure 2a, dashed line) because of nitric acid doping during the purification procedure.<sup>20</sup> Annealing of the purified material in vacuum at 350 °C for 90 min recovers the full strength of the  $S_{11}$  transition (Figure 2a, solid line).<sup>20</sup> Figure 2b shows a transmission spectrum of a sample taken at random from EA-produced AP-SWNTs material. As expected, the absorption bands  $S_{11}$ ,  $S_{22}$ , and  $M_{11}$  in the AP-SWNTs are less prominent than in the purified sample. Also shown in Figure 2a is the featureless transmission spectrum produced by a film of carbon black, which provides a representation of the spectral contribution of the carbonaceous impurities that arise in the EA production of AP-SWNT soot. The spectrum of the AP-

SWNTs (Figure 2b) is therefore a superposition of the spectra of pure SWNTs and carbonaceous impurities (Figure 2a). Given the availability of a pure SWNT reference sample, we can suggest a simple algorithm that allows the calculation of the absolute purity of AP-SWNT soot (Figure 2b) to be made by separating the contributions of the two components in Figure 2a. At the present time, a 100% pure reference sample of SWNTs is not available, so we chose to adopt as a reference the sample showing the highest purity.

The first candidate for the highest-purity (reference) material is the EA-produced SWNTs purified by the cross-flow filtration procedure.<sup>6,35</sup> A NIR spectrum of a thin film of this material is presented in Figure 2a, and we label this sample as reference number 1 (R1). As a second candidate for the highest-purity SWNT sample, we sought to obtain a sample directly from the arc chamber without any chemical processing. For this purpose, we placed a stainless steel wire grid of cell size 5 cm so that it surrounded the arc discharge area. During operation, the grid initiates the condensation of significant quantities of the SWNTs, and an extremely thin, homogeneous, and semitransparent weblike film is formed on parts of the grid. Several of the thinnest fragments of such films were transferred onto a glass substrate and analyzed by SEM and NIR spectroscopy. Figure 3a shows a view of one of the films on a glass slide imaged through an optical microscope. The SEM image of a fragment of this film (Figure 3b) appears to consist of SWNTs without any visible traces of impurities. This impurity-free fragment of soot may be the result of self-filtration during the arc discharge process. The arrays of SWNTs drift from the plasma area and become trapped by the grid and the growing network of SWNTs. The amorphous carbon and nanoparticles propagate ballistically to the walls of the chamber with a much lower chance of trapping. This is in agreement with previous findings that the weblike part of the AP-SWNT soot usually exceeds in quality the part collected from the walls of the chamber.<sup>5,23</sup> Figure 3c shows a NIR absorption spectrum taken directly on this film, which is labeled reference number 2 (R2), together with the spectrum of R1. It may be seen that the characteristic SWNT transitions  $S_{11}$ ,  $S_{22}$ , and  $M_{11}$  are more prominent in R2 than in R1. Thus, R2 is of higher purity than R1, and in our procedure, we adopt R2 as the reference material for the evaluation of the carbonaceous purity of AP-SWNT soot.

NIR transmission spectroscopy of SWNTs has been reported on thin films and on solution-phase samples.<sup>13,15,20,28–32,34</sup> However, the reproducible preparation of the SWNT films is difficult, and the control of film thickness is not a trivial task. The SWNTs have a tendency to aggregate into macrostructures during spraying, and this leads to scattering of the incident light and distortion of the spectral features, especially in the case of high optical densities. As a result, corrections to the spectral shape and band intensities are required,<sup>36</sup> which makes the purity evaluation procedure more complicated and less accurate. We found that solution-phase spectroscopy provided more accurate and reproducible data.

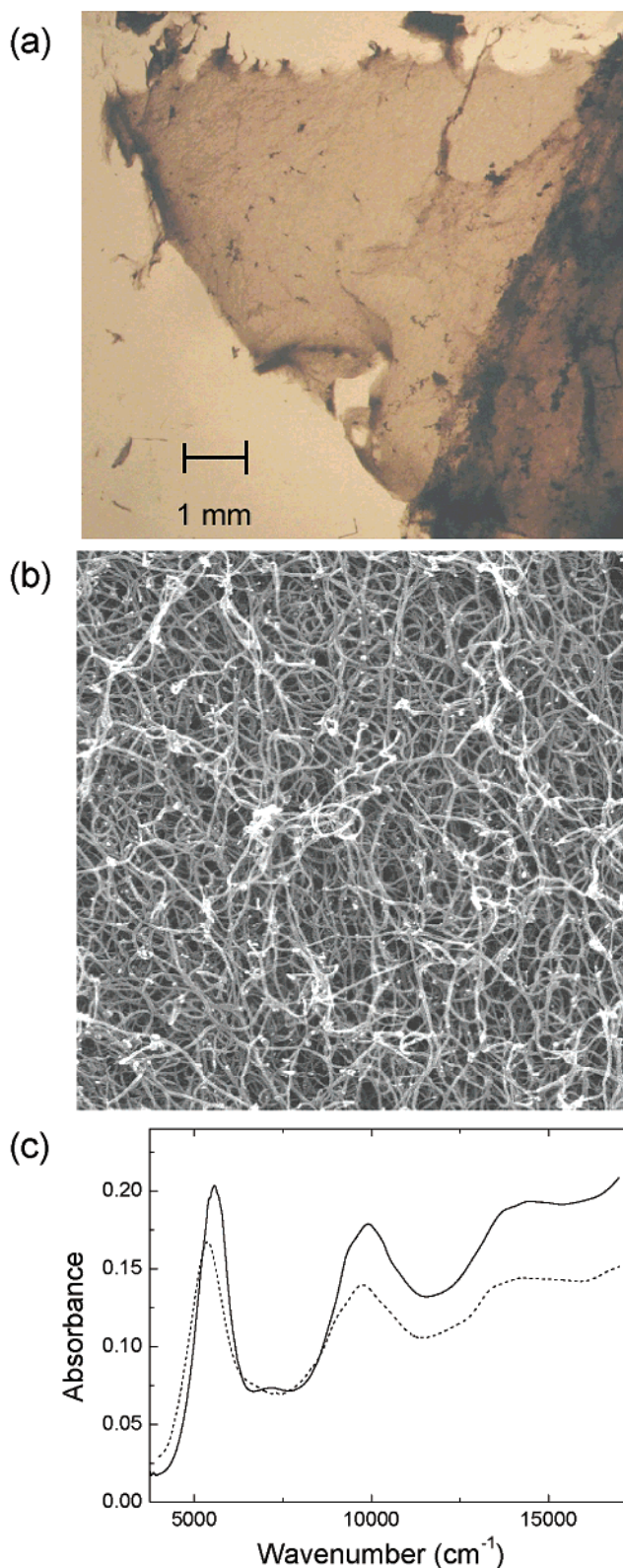


**Figure 3.** Semitransparent weblike film of AP-SWNT soot transferred from the arc chamber on a glass slide (a) imaged through an optical microscope; (b) SEM image of a fragment of this film; and (c) NIR absorption spectrum of this film (reference sample R2, solid line) in comparison with the spectrum of purified material (reference sample R1, dashed line)

Our procedure begins with a two-step homogenization process, which is required to obtain spectral data that

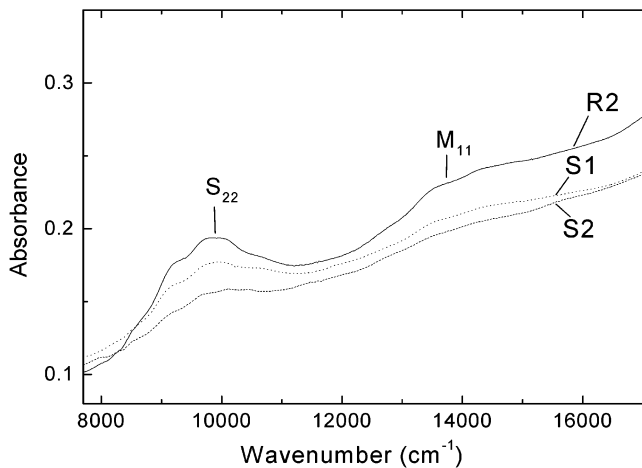


**Figure 4.** Absorption spectra of the reference sample R2 (—), and two samples of AP-SWNTs of different purity S1 (· ·) and S2 (— ·), dispersed in DMF.

represent the average purity of large batches of SWNTs. In the first step, 10 g of AP-SWNT soot is mechanically homogenized until a fine powder is obtained. In the second step, 50 mg of initially homogenized soot is dispersed in 100 mL of DMF by ultrasonication and mechanical stirring for 5 min. During this step, a homogeneous slurry of the AP-SWNT soot is obtained. Then, a few drops of the SWNT slurry were further dissolved in 10 mL of DMF to obtain a faintly colored nonscattering dispersion after an additional 2 min of ultrasonication. Sonication was minimized to avoid damage to the SWNTs during sample preparation. The concentration of the dispersion was adjusted to obtain an optical density in the range of 0.15–0.2 at 12 000 cm<sup>-1</sup>. We

estimate that this dispersion corresponds to a concentration of AP-SWNT soot in DMF of about 0.01 mg/mL; this concentration was found to give the optimum signal-to-noise ratio for recording the spectra. At higher concentrations, the dispersions were less stable, and under these circumstances, aggregation and light scattering lead to a distortion of the spectral features.

We chose DMF as a solvent for two reasons: first, it is capable of dispersing SWNTs with a minimal application of ultrasound, and second, it has a transmission window in the spectral range of 7500–35 000 cm<sup>-1</sup>, which allows the observation of the S<sub>22</sub> and M<sub>11</sub> interband transitions for the semiconducting SWNTs. Any of the prominent bands S<sub>11</sub>, S<sub>22</sub>, and M<sub>11</sub> can be used for the purity evaluation. The S<sub>11</sub> band would provide the most accurate measure of purity because it has the highest amplitude. However, the S<sub>22</sub> transition is much less affected by doping during chemical processing (Figure 2a),<sup>13,20,37</sup> so the current method is not susceptible to errors due to chemical processing of SWNTs that are to be evaluated for purity.

Figure 4 illustrates the NIR spectroscopic analysis of three samples, where R2 is the reference sample and S1 and S2 are bulk samples of different purity provided by Carbon Solutions, Inc. Figure 4 shows a broad scan of the NIR spectral region that includes the S<sub>22</sub> and M<sub>11</sub> transitions; strong DMF absorptions at lower energy preclude the observation of the S<sub>11</sub> transition in this solvent. Figure 5a–c shows the NIR absorption spectra corresponding to the S<sub>22</sub> band for reference R2 (set to 100% purity; Figure 4a) and the samples for which the purity is to be evaluated (S1 and S2 in Figure 5b and c, respectively). Figure 5a–c shows the S<sub>22</sub> absorptions after linear baseline subtraction (upper frame,

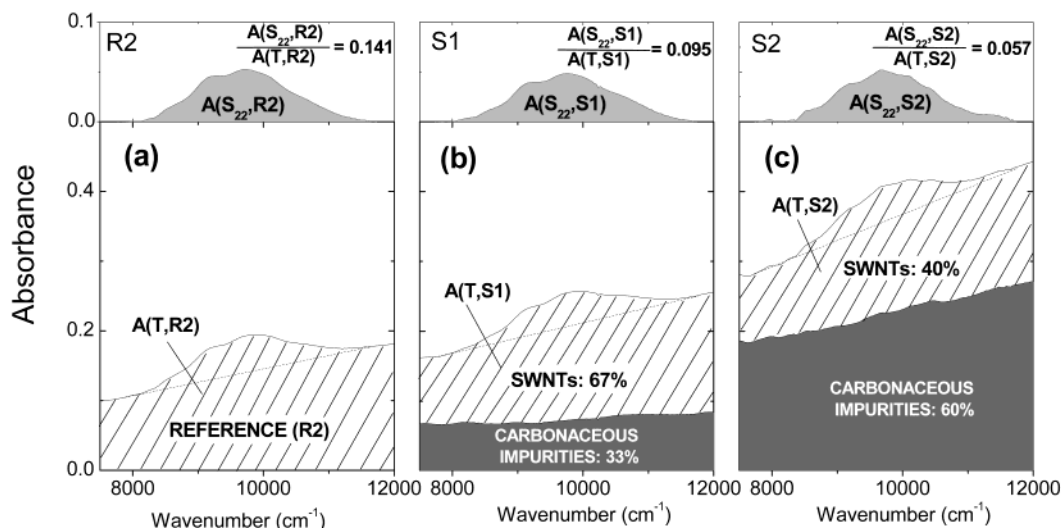


**Figure 5.** (a) Absorption spectrum of reference sample R2 in DMF in the range of the S<sub>22</sub> interband transition before (bottom frame) and after (top frame) baseline subtraction. The ratio of the areas under the curves in the top and bottom frames,  $A(S_{22}, R2)/A(T, R2)$  is equal to 0.141. (b) Absorption spectrum of AP-SWNT sample S1 in DMF before (bottom frame) and after (top frame) baseline subtraction. The ratio of the areas under the curves in the top and bottom frames,  $A(S_{22}, S1)/A(T, S1)$  is equal to 0.095. Thus, the carbonaceous purity of sample S1 is estimated to be 67% (0.095/0.141) against the R2 reference sample. (c) Absorption spectrum of AP-SWNT sample S2 of lower purity than S1 in DMF before (bottom frame) and after (top frame) baseline subtraction. The ratio of the areas under the curves in the top and bottom frames,  $A(S_{22}, S2)/A(T, S2)$  is equal to 0.057. Thus, the carbonaceous purity of sample S1 is estimated to be 40% (0.057/0.141) against the R2 reference sample. The absorption spectra in frames b and c are scaled so that the areas under the peaks  $A(S_{22}, S1)$  and  $A(S_{22}, S2)$  match the area under the peak of the reference sample  $A(S_{22}, R2)$  in frame a. Hatched areas correspond to the SWNT contribution whereas the shaded area in the bottom frames corresponds to the contribution of the carbonaceous impurities.

scaled to the area of  $A(S_{22}, R2)$ ). The carbonaceous purity  $[P(S1)]$  of the S1 AP-SWNT sample against R2 is calculated by integrating the areas under the curves for the spectra in Figure 5b and c and evaluating the expression

$$P(S1) = \frac{[A(S_{22}, S1)/A(T, S1)]}{[A(S_{22}, R2)/A(T, R2)]} \times 100 \quad (1)$$

where  $A(T, S1)$  and  $A(T, R2)$  are the total areas under the spectral curves given in Figure 5b and c and  $A(S_{22}, S1)$  and  $A(S_{22}, R2)$  are the areas under the  $S_{22}$  absorptions in Figure 5b and a for S1 and reference R2 samples, respectively. Equation 1 corresponds to the ratio of the hatched area (SWNT contribution) to the total area under the spectral curves in Figure 5a–c. Note that  $A(S_{22}, R2)/A(T, R2)$  is equal to 0.141, the highest value that we have observed so far for an EA-produced AP-SWNT sample dispersed in DMF. For the particular case of the EA synthesis with a Ni/Y catalysts ratio of 4:1 atomic %, spectral cutoffs of 7750 and 11 750  $\text{cm}^{-1}$  were chosen for the spectral window for the integration of the spectra and the baseline correction. This cutoff is applicable to the majority of commercially available EA-produced SWNT soot. For SWNTs with a different diameter distribution, it will be necessary to modify the spectral cutoffs so as to capture the  $S_{22}$  absorptions that are known to have energies that are an inverse function of the diameter.<sup>28,34,38</sup> In our calculation, we assume that every carbon atom makes the same contribution to the area under the spectral curves in this region of the spectrum. In this case, the value of the expression  $A(T, R2) \cdot [A(S_{22}, S1)/A(S_{22}, R2)]$  represents the part of the total absorption  $A(T, S1)$  of AP-SWNTs that originates from the SWNTs whereas the value of the expression  $A(T, S1) - A(T, R2) \cdot [A(S_{22}, S1)/A(S_{22}, R2)]$  gives the contribution of the carbonaceous impurities shaded in the bottom of Figure 5b and c. The spectral curve for the carbonaceous impurities is featureless and is similar to the spectrum of carbon black (Figure 2a). The metallic impurities are not taken into account in this analysis and can contribute from 10 to 30 wt % of sample but only 2 to 5 volume %. Thus, for a complete evaluation of AP-SWNT soot purity over all elements, it is necessary to evaluate the metal impurities in a separate experiment such as TGA.

It should be noted that the spectrum of a thin film of material shows stronger SWNT features than the spectrum of the same sample dispersed in DMF; this medium effect is caused by the high polarizability of the DMF.<sup>39</sup> Because of this effect, for quantitative purity evaluation the AP-SWNT sample must be tested in the same phase as the reference sample.

In the procedure given above, the NIR spectroscopy is effectively carried out on a 0.1-mg sample of the AP-SWNT soot (10 mL of a 0.01 mg/mL dispersion), which should represent the purity of the full 10-g batch if the homogenization procedure is effective. To test the accuracy and reliability of this purity evaluation procedure, we carried out independent purity evaluations on five different random 50-mg samples of AP-SWNT soot after the completion of the first step of mechanical homogenization of the 10-g batch of AP-

**Table 1**

sample	1	2	3	4	5	mean value (SD)
purity, %	31.8	36.5	34.3	36.4	34.4	34.5 ( $\pm 1.8$ )

SWNTs. (Reference sample R2 was also taken from this batch.) The results are shown in Table 1 and clearly demonstrate the efficiency and reliability of the procedure in evaluating the bulk carbonaceous purity of SWNT samples.

In summary, we have presented a practical procedure for the quantitative evaluation of the purity of bulk quantities of AP-SWNT soot on the basis of NIR spectroscopy. This procedure can be used to monitor the quality of AP-SWNT soot, thus allowing the optimization of the EA parameters. The method can also be utilized for the evaluation of the efficiency of purification techniques, for monitoring the effects of chemical functionalization of the SWNTs, and also in identifying the different types of SWNTs that are present in a sample.<sup>40</sup>

**Acknowledgment.** This work was supported by the MRSEC Program of the National Science Foundation under Award No. DMR-9809686 and by DOD/DARPA/DMEA under Award No. DMEA90-02-2-0216. Carbon Solutions, Inc. acknowledges NSF SBIR Phase I and II Awards No. DMI-0110221 from the Division for Design, Manufacture and Industrial Innovation.

## References

- (1) Dresselhaus, M. S.; Dresselhaus, G.; Avouris, P. *Carbon Nanotubes: Synthesis, Structure, Properties and Applications*; Springer-Verlag: Berlin, 2001; Vol. 80.
- (2) Avouris, P. *Acc. Chem. Res.* **2002**, *35*, 1026–1034.
- (3) Dai, H. *Acc. Chem. Res.* **2002**, *35*, 1035–1044.
- (4) Niyogi, S.; Hamon, M. A.; Hu, H.; Zhao, B.; Bhowmik, P.; Sen, R.; Itkis, M. E.; Haddon, R. C. *Acc. Chem. Res.* **2002**, *35*, 1105–1113.
- (5) Journet, C.; Maser, W. K.; Bernier, P.; Loiseau, A.; Lamy de la Chappelle, M.; Lefrant, S.; Deniard, P.; Lee, R.; Fischer, J. E. *Nature (London)* **1997**, *388*, 756–758.
- (6) Rinzler, A. G.; Liu, J.; Dai, H.; Nilolaev, P.; Huffman, C. B.; Rodriguez-Macias, F. J.; Boul, P. J.; Lu, A. H.; Heymann, D.; Colbert, D. T.; Lee, R. S.; Fischer, J. E.; Rao, A. M.; Eklund, P. C.; Smalley, R. E. *Appl. Phys. A* **1998**, *67*, 29–37.
- (7) Nikolaev, P.; Bronikowski, M. J.; Bradley, R. K.; Rohmund, F.; Colbert, D. T.; Smith, K. A.; Smalley, R. E. *Chem. Phys. Lett.* **1999**, *313*, 91–97.
- (8) Zhou, W.; Ooi, Y. H.; Russo, R.; Papanek, P.; Luzzi, D. E.; Fischer, J. E.; Bronikowski, M. J.; Willis, P. A.; Smalley, R. E. *Chem. Phys. Lett.* **2001**, *350*, 6–14.
- (9) Chiang, I. W.; Brinson, B. E.; Huang, A. Y.; Willis, P. A.; Bronikowski, M. J.; Margrave, J. L.; Smalley, R. E.; Hauge, R. H. *J. Phys. Chem. B* **2001**, *105*, 8297–8301.
- (10) Harutyunyan, A. R.; Pradhan, B. K.; Chang, J.; Chen, G.; Eklund, P. C. *J. Phys. Chem. B* **2002**, *106*, 8671–8675.
- (11) Chiang, I. W.; Brinson, B. E.; Smalley, R. E.; Margrave, J. L.; Hauge, R. H. *J. Phys. Chem. B* **2001**, *105*, 1157–1161.
- (12) Moon, J. M.; An, K. H.; Lee, Y. H.; Park, Y. S.; Bae, D. J.; Park, G. S. *J. Phys. Chem. B* **2001**, *105*, 5677–5681.
- (13) Chen, J.; Hamon, M. A.; Hu, H.; Chen, Y.; Rao, A. M.; Eklund, P. C.; Haddon, R. C. *Science (Washington, D.C.)* **1998**, *282*, 95–98.
- (14) Bower, C.; Kleinhammes, A.; Wu, Y.; Zhou, O. *Chem. Phys. Lett.* **1998**, *288*, 481.
- (15) Petit, P.; Mathis, C.; Journet, C.; Bernier, P. *Chem. Phys. Lett.* **1999**, *305*, 370–374.

- (16) Kazaoui, S.; Minami, N.; Jacquemin, R.; Kataura, H.; Achiba, Y. *Phys. Rev. B* **1999**, *60*, 13339–13342.
- (17) Kuznetsova, A.; Mawhinney, D. B.; Naumenko, V.; Yates, J. T., Jr.; Liu, J.; Smalley, R. E. *Chem. Phys. Lett.* **2000**, *321*, 292–296.
- (18) Kuznetsova, A.; Popova, I.; Yates, J. T.; Bronikowski, M. J.; Huffman, C. B.; Liu, J.; Smalley, R. E.; Hwu, H. H.; Chen, J. G. *J. Am. Chem. Soc.* **2001**, *123*, 10699–10704.
- (19) Hu, H.; Bhowmik, P.; Zhao, B.; Hamon, M. A.; Itkis, M. E.; Haddon, R. C. *Chem. Phys. Lett.* **2001**, *345*, 25–28.
- (20) Itkis, M. E.; Niyogi, S.; Meng, M.; Hamon, M.; Hu, H.; Haddon, R. C. *NanoLett.* **2002**, *2*, 155–159.
- (21) Huang, H.; Marie, J.; Kajiuira, H.; Ata, M. *Nano Lett.* **2002**, *2*, 1117–1119.
- (22) Yudasaka, M.; Sensui, N.; Takizawa, M.; Bandow, S.; Ichihashi, T.; Ijima, S. *Chem. Phys. Lett.* **1999**, *312*, 155–160.
- (23) Kajiuira, H.; Tsutsui, S.; Huang, H.; Miyakoshi, M.; Hirano, Y.; Yamada, A.; Ata, M. *Chem. Phys. Lett.* **2001**, *346*, 356–366.
- (24) Takizawa, M.; Bandow, S.; Torii, T.; Ijima, S. *Chem. Phys. Lett.* **1999**, *302*, 146–150.
- (25) Dillon, A. C.; Gennett, T.; Parilla, P. A.; Alleman, J. L.; Jones, K. M.; Heben, M. J. *Mater. Res. Soc. Symp. Proc.* **2001**, *633*, A5.2.1–A5.2.6.
- (26) Dillon, A. C.; Gennett, T.; Jones, K. M.; Alleman, J. L.; Parilla, P. A.; Heben, M. J. *Adv. Mater.* **1999**, *11*, 1354–1358.
- (27) Terekhov, S. V.; Obratsova, E. D.; Lobach, A. S.; Konov, V. I. *Appl. Phys. A* **2002**, *74*, 393–396.
- (28) Kataura, H.; Kumazawa, Y.; Maniwa, Y.; Umezumi, I.; Suzuki, S.; Ohtsuka, Y.; Achiba, Y. *Synth. Met.* **1999**, *103*, 2555–2558.
- (29) Kazaoui, S.; Minami, N.; Jacquemin, R.; Kataura, H.; Achiba, Y. *Phys. Rev. B* **2001**, *60*, 13339–13342.
- (30) Kavan, L.; Rapta, P.; Dunsch, L.; Bronikowski, M. J.; Willis, P.; Smalley, R. E. *J. Phys. Chem. B* **2001**, *105*, 10764–10771.
- (31) Jost, O.; Gorbunov, A. A.; Pompe, W.; Pichler, T.; Friedlein, R.; Knupfer, M.; Reibold, M.; Bauer, H.-D.; Dunsch, L.; Golden, M. S.; Fink, J. *Appl. Phys. Lett.* **1999**, *75*, 2217–2219.
- (32) Liu, X.; Pichler, T.; Knupfer, M.; Golden, M. S.; Fink, J.; Kataura, H.; Achiba, Y. *Phys. Rev. B* **2002**, *66*, 045411.
- (33) Ouyang, M.; Huang, J.-L.; Lieber, C. M. *Acc. Chem. Res.* **2002**, *35*, 1018–1025.
- (34) Hamon, M. A.; Itkis, M. E.; Niyogi, S.; Alvaraez, T.; Kuper, C.; Menon, M.; Haddon, R. C. *J. Am. Chem. Soc.* **2001**, *123*, 11292–11293.
- (35) Liu, J.; Rinzler, A. G.; Dai, H.; Hafner, J. H.; Bradley, R. K.; Boul, P. J.; Lu, A.; Iverson, T.; Shelimov, K.; Huffman, C. B.; Rodriguez-Macias, F.; Shon, Y.-S.; Lee, T. R.; Colbert, D. T.; Smalley, R. E. *Science (Washington, D.C.)* **1998**, *280*, 1253–1255.
- (36) Jost, O.; Gorbunov, A. A.; Moller, J.; Pompe, W.; Lui, X.; Georgi, P.; Dunsch, L.; Golden, M. S.; Fink, J. *J. Phys. Chem. B* **2002**, *106*, 2875–2883.
- (37) Hamon, M. A.; Chen, J.; Hu, H.; Chen, Y.; Rao, A. M.; Eklund, P. C.; Haddon, R. C. *Adv. Mater.* **1999**, *11*, 834–840.
- (38) Dresselhaus, M. S.; Dresselhaus, G.; Eklund, P. C. *Science of Fullerenes and Carbon Nanotubes*; Academic Press: San Diego, CA, 1996.
- (39) Sullivan, D. E.; Deutch, J. M. *J. Chem. Phys.* **1976**, *65*, 5315–5317.
- (40) Bachilo, S. M.; Strano, M. S.; Kittrell, C.; Hauge, R. H.; Smalley, R. E.; Weisman, R. B. *Science (Washington, D.C.)* **2002**, *298*, 2361–2366.

NL025926E